(Received 4 April 2025, Accepted 26 May 2025, Scheduled 17 June 2025)

Improved Terminal Sliding Mode Control of PMSM Dual-Inertia System with Acceleration Feedback Based on Finite-Time ESO

Yingshen He[1], Kaihui Zhao[1,*], Zhixuan Yi[1], and Yishan Huang[2]

[1]*School of Transportation and Electrical Engineering, Hunan University of Technology, China*
[2]*CRRC Electric Vehicle Co., Ltd., China*

ABSTRACT: When permanent magnet synchronous motors (PMSMs) drive flexible loads, unknown disturbances (such as sudden load torque changes, parameter uncertainties, and unmodeled dynamics) can degrade the control performance of the system and may even cause irreversible physical damage. To deal with this problem, this paper presents an improved non-singular terminal sliding mode control (INTSMC) scheme based on a finite-time extended state observer. First, the acceleration feedback is introduced into the speed loop to establish the dual-inertia model of the PMSM flexible load system. Secondly, the conventional exponential reaching law is improved to obtain a novel reaching law with adaptive adjustment of the convergence speed, and a novel INTSMC controller is designed accordingly to enhance the system response speed. Then, a finite-time extended state observer (FTESO) is designed to estimate the disturbances of the system, and the estimated disturbances are compensated for the INTSMC controller to achieve convergence in finite time and improve the robustness of the system. The finite-time stability theory is used to prove the stability of the designed controller and observer. Finally, the simulations and experiments demonstrate the effectiveness of the proposed control scheme in improving the system's anti-disturbance capability.

1. INTRODUCTION

In high-performance motion control systems, PMSMs are typically coupled to the load via a flexible transmission mechanism [1]. The speed and angular displacement differences between the motor and load can easily occur with high-gain control conditions. Furthermore, motor parameter variations and unknown external disturbances may induce system resonance, thereby degrading control performance.

The motor drive and load systems are commonly modeled as dual-inertia systems interconnected by flexible couplings. To improve system performance, various control strategies have been proposed, such as active disturbance rejection control [2, 3], proportional-integral (PI) control [4], adaptive control [5], model predictive control [6], and sliding mode control (SMC) [7]. Conventional linear SMC is widely employed due to its robustness, fast dynamic response, and excellent disturbance rejection capabilities. However, conventional linear SMC only achieves asymptotic convergence. Moreover, the inherent discontinuity of the switching function often induces system chattering [8].

In contrast, terminal SMC (TSMC) makes the system state converge to zero in a finite time. For instance, an integral TSMC strategy was proposed for uncertain nonlinear systems to ensure that the system state starts on the sliding surface, thus eliminating the reaching time and achieving finite-time convergence [9]. Similarly, a discrete TSMC was proposed to enhance the system's dynamic and static characteristics as well as its resistance to disturbances [10]. However, TSMC exhibits a singular phenomenon. Nonsingular TSMC (NTSMC) solves the singularity problem, but it converges slowly when the system state is far away from the point of equilibrium [11]. Nonsingular fast TSMC (FTSMC) solves the singularity problem and accelerates the convergence of the TSMC [12]. Furthermore, a nonlinear variable-gain NFTSMC was developed that incorporated a nonlinear function with variable parameters into the TSMC to improve response speed and reduce chattering [13].

Uncertainty disturbances are often difficult to measure directly in PMSM dual-inertia systems. Extended state observer (ESO) is commonly used to estimate these disturbances. The core idea of ESO is to consider unknown disturbances as an extended state and design an observer to estimate and compensate them, thus enhancing the system's robustness [14]. However, ESO is ambiguous in its design, and its convergence is not guaranteed theoretically. To overcome these limitations, ESO has been continuously improved. Two adaptive ESOs are designed to estimate back electromotive forces (EMFs) and achieve sensorless PMSM control [15]. A finite-time convergent ESO was proposed, combined with a homogenous controller for disturbance compensation to improve tracking performance and ensure finite-time convergence [16]. Integrating finite-time stability techniques into the design of ESO enables rapid and precise estimation of states and disturbances within a finite time [17].

In addition to designing the ESO, integrating compensation algorithms, such as acceleration feedback, into the controller can also compensate disturbances. Acceleration feedback was used for the control of launch vehicles by constructing an ESO to compensate wind disturbances and uncertain aerodynam-

* Corresponding author: Kaihui Zhao (zhaokaihui@hut.edu.cn).

ics [18], but this approach resulted in insufficient dynamic response. The acceleration feedback was introduced in the speed loop, and NTSMC was designed to reduce the effect of mechanical resonance in PMSM dual-inertia systems [19], but this method was validated only through simulation. An SMC based on finite-time ESO (FTESO) was designed to improve the anti-disturbance property of PMSM [20], but the influence of the rotational inertia of the load was not taken into account.

This paper proposes an improved NTSMC (INTSMC) approach based on finite-time ESO (hereafter referred to as the FTESO-based INTSMC approach, i.e., the INTSMC+FTESO approach). The approach incorporates motor acceleration feedback into the speed loop to improve the robustness of a PMSM dual-inertia system with uncertain disturbances. The FTESO-based INTSMC approach is compared with the NTSMC based on a conventional ESO (hereafter referred to as the NTSMC+ESO approach) and proportional-integral (PI) control.

The main contributions of this article are as follows:

(i) We combine INTSMC and FTESO methods to improve the performance of a PMSM dual-inertia system. More specifically, FTESO ensures accurate estimation of unknown disturbances, and INTSMC improves the robustness of the system to unknown disturbances.

(ii) We design an FTESO that combines the advantages of a finite-time observer and a conventional ESO. It not only observes the system state, but also provides feedback and compensates disturbances. This design ensures fast convergence of the tracking error in finite time while significantly enhancing the robustness of the system.

(iii) We utilize the concept of finite-time convergence to demonstrate the stability of the designed method and solve for the convergence time of the system. Then, the effectiveness and superiority of the proposed approach are verified by simulation and experiment.

This paper is structured as follows. Section 2 presents the mathematical model of the PMSM dual-inertia system with acceleration feedback. Section 3 describes the INTSMC approach and includes the design and stability proofing of the speed loop controller. Section 4 develops an FTESO and demonstrates its stability using the finite-time stability theorem. The validity of the proposed approach is verified through simulation and experimentation in Section 5. Finally, Section 6 concludes the paper.

2. MATHEMATICAL MODELLING OF PMSM DUAL-INERTIA SYSTEMS

This section presents the dynamic model of the PMSM dual-inertia system with the introduction of acceleration feedback, which will be used to design the INTSMC in the next section.

The PMSM drags the load through the flexible transmission mechanism, which has a certain stiffness coefficient and damping coefficient. When the motor drives the load, the torsional deformation occurs on the flexible transmission mechanism and generates torque. Compared with the motor and load, the inertia of the flexible transmission mechanism is very small, so it is negligible. Then, the flexible transmission mechanism between the motor and load is equivalent to the dual-inertia system model shown in Fig. 1.

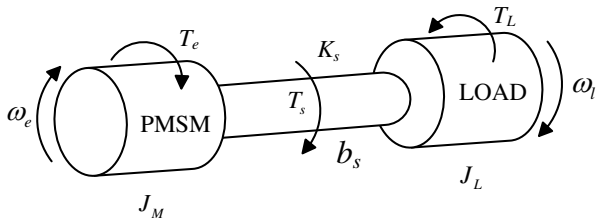

FIGURE 1. PMSM dual-inertia system.

In Fig. 1, J_M is the rotational inertia of the motor; J_L is the moment of inertia of the load; ω_m is the mechanical angular velocity of the motor; ω_L is the angular velocity of the load; b_s is the torsional damping coefficient; K_s is the stiffness coefficient; T_e is the electromagnetic torque; T_L is the load torque; T_s is the shaft torque.

The introduction of acceleration feedback in the speed loop is equivalent to increasing the rotational inertia of the motor from J_M to $J_M\left(1+G_{VD}\right)$. In practical engineering, it does not increase the size and weight of the motor, and increases the active damping of the system, which is conducive to the suppression of chattering vibration [19].

The mathematical model of the PMSM dual-inertia system with acceleration feedback in the *d-q* axis is:

$$\begin{cases} \dfrac{di_d}{dt} = \left(\omega_e i_q L_q - R_s i_d + u_d\right)\dfrac{1}{L_d} \\ \dfrac{di_q}{dt} = \left(-\omega_e i_d L_d - R_s i_q - \omega_e \psi_r + u_q\right)\dfrac{1}{L_q} \\ \dfrac{d\omega_e}{dt} = \dfrac{\left[p_n^2 \psi_r i_q - b_s\left(\omega_e - \omega_l\right) - K_s\left(\theta_e - \theta_l\right)\right]}{J_M\left(1+G_{VD}\right)} \\ \dfrac{d\omega_l}{dt} = \left[b_s\left(\omega_e - \omega_l\right) + K_s\left(\theta_e - \theta_l\right) - T_L p_n\right]\dfrac{1}{J_L} \\ \dot{\theta}_e = \omega_e \\ \dot{\theta}_l = \omega_l \end{cases} \tag{1}$$

where

$u_d,\ u_q$: *d-q* axis stator voltage (V);
$i_d,\ i_q$: *d-q* axis stator current (A);
$L_d,\ L_q$: *d-q* axis nominal stator inductance (H);
R_s: stator resistance (Ω);
ψ_r: amplitude of PM flux (Wb);
ω_e: electrical angular velocity of the motor side (rad/s), $\omega_e = p_n\omega_m$;
ω_l: electrical angular velocities of the load side (rad/s), $\omega_l = p_n\omega_L$;
θ_e: electrical angular of the motor side (rad), $\theta_e = p_n\theta_m$;
θ_l: electrical angular of the load side (rad), $\theta_l = p_n\theta_L$;
p_n: number of pole pairs;

G_{VD}: acceleration feedback gain.

The motor side electrical angular acceleration, a_1, is

$$a_1 = \frac{\mathrm{d}\omega_e}{\mathrm{d}t} \tag{2}$$

The load side electrical angular acceleration is defined as a_2.

Selecting the state variable $x = [x_1\ x_2]^{\mathrm{T}} = [\theta_e\ \omega_e]^{\mathrm{T}} \in R^2$, the mechanical equation of motion of the motor side is expressed as

$$\begin{cases} \dot{x}_1 = x_2 \\ \dot{x}_2 = ax_2 + bu + d \end{cases} \tag{3}$$

where $a = \frac{-b_s}{J_M(1+G_{VD})}$, $b = \frac{p_n^2\psi_{\mathrm{r}}}{J_{\mathrm{M}}(1+G_{VD})}$, $d = \frac{b_s\omega_l - K_s(\theta_e-\theta_l)}{J_M(1+G_{VD})}$, $u = i_{\mathrm{q}}$.

Considering the unknown disturbances in practical applications, (3) is rewritten as

$$\begin{cases} \dot{x}_1 = x_2 \\ \dot{x}_2 = (a+\Delta a_0)x_2 + (b+\Delta b_0)u + (d+\Delta d_0) \\ \quad = a_0x_2 + b_0u + h \end{cases} \tag{4}$$

where a_0, b_0, d_0 are the nominal values of a, b, d, respectively; Δa_0, Δb_0, Δd_0 are the parameter perturbation values; and h is the unknown lumped disturbance.

Assumption 1 *The unknown lumped disturbance h is continuously differentiable with respect to time.*

Assumption 2 *The rate of change of the lumped disturbance is unknown but bounded. This means that the following inequality holds.*

$$\left|\dot{h}\right| \le \dot{\bar{h}} \tag{5}$$

where $\dot{\bar{h}}$ is a known upper bound of the change rate of disturbance $\dot{h}$.

3. DESIGN OF INTSMC

In this section, we propose an INTSMC method based on the improved exponential reaching law, and the stability is proved. Then, the controller is designed to regulate the speed loop of the PMSM dual-inertia system.

Define the electrical angular velocity tracking error as:

$$e = \omega_e^* - \omega_e \tag{6}$$

where ω_e^* is the given electrical angular velocity of the motor.

An NTSM surface is used to ensure the finite-time convergence of the system:

$$s_1 = e + \gamma_1 \dot{e}^{p/q} \tag{7}$$

where $\gamma_1 > 0$, and p and q are both odd numbers greater than 0, $q < p$.

Derivation of (7) gives:

$$\dot{s}_1 = \dot{e} + \gamma_1 \ddot{e}^{p/q} \tag{8}$$

Using the conventional exponential reaching law $\dot{s} = -\varepsilon \mathrm{sign}(s) - ks\,(\varepsilon > 0, k > 0)$, the NTSMC control law is obtained as:

$$\begin{aligned} u_{smc1} =& \frac{1}{b_0}\int_0^t (-a_0\dot{x}_2 + \varepsilon \mathrm{sign}(s_1) + ks_1)d\tau \\ & - \frac{1}{b_0}\int_0^t \left(\dot{\hat{h}} - \frac{q}{\gamma_1 p}\dot{e}^{2-p/q}\right)d\tau \end{aligned} \tag{9}$$

where $\hat{h}$ is the estimated disturbance, and its derivative $\dot{\hat{h}}$ is a bounded quantity.

However, the conventional exponential reaching law exhibits two critical deficiencies: suboptimal convergence and inadequate chattering suppression. Therefore, we design an improved exponential reaching law which adaptively adjusts the convergence rate:

$$\begin{cases} \dfrac{\mathrm{d}s}{\mathrm{d}t} = -\lambda f(s)\mathrm{sign}(s) - k_2 s \\ f(s) = \dfrac{k_1}{1/[\ln(|s| + \mathrm{e})]^{\eta} + k_1/(|s|+1)} \end{cases} \tag{10}$$

where λ, k_1, k_2 are greater than 0, $\eta > 1$, and e is a natural constant.

Remark 1 *The reaching law is based on the exponential reaching law and introduces a polynomial function. This function combines the absolute value of the sliding mode surface function $|s|$. Therefore, the reaching law achieves adaptive speed adjustment based on the proximity of the state and the sliding mode surface, thereby reducing convergence time.*

From (4) and (10), INTSMC control law is designed as:

$$\begin{aligned} u_{smc2} =& \frac{1}{b_0}\int_0^t (-a_0\dot{x}_2 + \lambda f(s_1)\mathrm{sign}(s_1) + k_2 s_1)\,d\tau \\ & + \frac{1}{b_0}\int_0^t \left(\frac{q}{\gamma_2 p}\dot{e}^{2-p/q} - \dot{\hat{h}}\right)d\tau \end{aligned} \tag{11}$$

The sliding surface gain of INTSMC is γ_2. As can be seen from (11), the estimated disturbance is fed back into the control law to attenuate their effect on the system. Figure 2 shows the diagram of the designed INTSMC.

Theorem 1 *Choosing the sliding mode surface (7), selecting the reaching law (10), and designing the sliding mode control law (11), the state error variables converge in finite time.*

Proof 1 *The Lyapunov function is chosen as:*

$$V_1 = \frac{1}{2}s_1^2 \tag{12}$$

Derivation of (12) leads to (13):

$$\begin{aligned} \dot{V}_1 &= s_1\dot{s}_1 = s_1\left[\dot{e} + \gamma_2\,(p/q)\,\dot{e}^{p/q-1}\ddot{e}\right] \\ &\le -\gamma_2\,(p/q)\left[k_2 s_1^2 + \left(\lambda f\,(s_1) + \dot{\hat{h}}\right)|s_1|\ \right]\dot{e}^{p/q-1} \\ &\le -\eta_1 V_1^{1/2} - \eta_2 V_1 \le 0 \end{aligned} \tag{13}$$

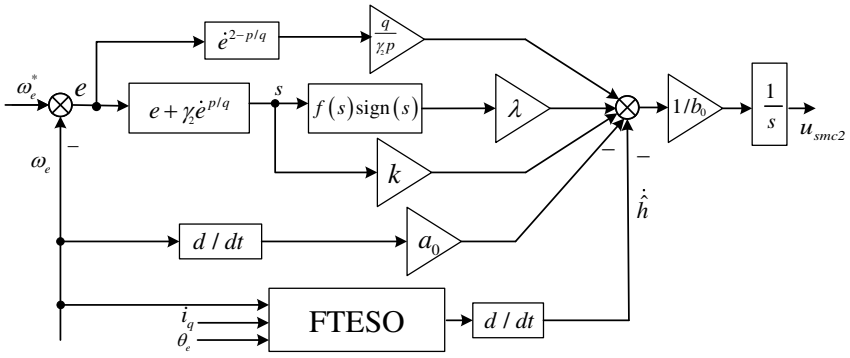

FIGURE 2. Block diagram of INTSMC.

where $\eta_1 = \sqrt{2}\gamma_2\left[\lambda f(s_1) + \dot{\hat{h}}\right](p/q)\,\dot{e}^{p/q-1}$, $\eta_2 = \gamma_2(p/q)\,\dot{e}^{p/q-1}k_2$.

Multiplying both sides of (13) by $0.5V_1^{-1/2}$, *we get*

$$\frac{\mathrm{d}V_1^{1/2}}{dt} + 0.5\eta_2 V_1^{1/2} \le -0.5\eta_1 \tag{14}$$

Multiplying both sides of (14) by $\mathrm{e}^{0.5\eta_2 t}$ *yields*

$$\frac{\mathrm{d}\left(\mathrm{e}^{0.5\eta_2 t}V_1^{1/2}\right)}{\mathrm{d}t} \le -\frac{1}{2}\eta_1\mathrm{e}^{0.5\eta_2 t} \tag{15}$$

Let $V_1(t_1) = 0$ *and integrating both sides of (15) simultaneously from time 0 to time* t_1, *we get*

$$-\mathrm{e}^{0.5\eta_2 t}V_1^{1/2}(0) \le -\frac{\eta_1}{\eta_2}\left(\mathrm{e}^{0.5\eta_2 t_1} - 1\right) \tag{16}$$

The convergence time of the sliding mode surface is solved as:

$$t_1 \le \frac{2}{\eta_2}\ln\left(1 + \frac{\eta_1}{\eta_2}V_1^{1/2}(0)\right) \tag{17}$$

Construct the Lyapunov function as

$$V_2 = \frac{1}{2}e^2 \tag{18}$$

Derivation of (18) yields

$$\dot{V}_2 = -e\left(\frac{e}{\gamma_2}\right)^{q/p} \le -\sqrt{2}\left|\frac{e}{\gamma_2}\right|^{q/p}V_2^{1/2} \le 0 \tag{19}$$

Shifting the terms of (19) yields

$$\dot{V}_2 + \sqrt{2}\left|\frac{e}{\gamma_2}\right|^{q/p}V_2^{1/2} \le 0 \tag{20}$$

Finally, from (20), the variable e *converges in finite time* $t_2 \le \sqrt{2}\left|\frac{e}{\gamma_2}\right|^{-q/p}V_2^{1/2}(0)$.

To solve the sliding mode chattering problem caused by the switching function $\mathrm{sign}(s)$, the continuous function $\mathrm{sign}(s) = s/(|s| + \sigma)$ is used to replace the switching function, where σ is a smaller positive number.

4. DESIGN OF FTESO

This section designs an FTESO to make the estimation error of the unknown disturbances converge in finite time and feed the estimated unknown disturbances back to the controller to reduce its effect.

The conventional ESO is

$$\begin{cases}\dot{\hat{x}}_2 = a_0\hat{x}_2 + \hat{h} - \beta_0(\hat{x}_2 - x_2) + b_0u\\ \dot{\hat{h}} = -\beta_1(\hat{x}_2 - x_2)\end{cases} \tag{21}$$

where β_0 and β_1 are positive numbers.

Remark 2 *Conventional ESO is usually unable to respond to unknown disturbances in a finite time, thus affecting the performance of the controller.*

Remark 3 *Finite-time control techniques can provide faster convergence and better anti-disturbance performance. To further improve the response speed of the PMSM dual-inertia system and effectively suppress chattering, an FTESO is designed based on the ESO.*

The mechanical equations are rewritten so that $\hat{\theta}_e$, $\hat{\omega}_e$, and $\hat{h}$ denote the estimated values of the state variables θ_e, ω_e, and the lumped disturbance h, respectively. The state equations of the FTESO is obtained as:

$$\begin{cases}\dot{\hat{x}}_1 = \hat{x}_2 - c_1\mathrm{sig}(\hat{x}_1 - x_1)^{1/2}\\ \dot{\hat{x}}_2 = a_0\hat{x}_2 + b_0u - c_2\mathrm{sig}(\hat{x}_1 - x_1)\end{cases} \tag{22}$$

where $\mathrm{sig}(\cdot)^\eta = \mathrm{sign}(\cdot)|\cdot|^\eta$, $\eta > 0$, c_1, c_2 are the gains of FTESO to be designed. By choosing the appropriate observer gain, the lumped disturbance can be accurately estimated.

Lemma 1 *[21] Suppose that* $V : D \to R$ *is a continuous function that satisfies:*

(i) V *is positive definite;*

(ii) There exist real numbers $c > 0$, $g \in [0,1]$, $\alpha \in (0,1)$, $0 < \varsigma < \infty$, *and an open region* $U \subseteq D$ *near the origin such that:*

$$\dot{V}(x,t) \le -cV(x,t)^{\alpha} + \varsigma, x(t) \in U\backslash\{0\}.$$

Then, the system stabilizes in finite time. The convergence time is

$$T^* \le \frac{1}{cg(1-\alpha)} V^{1-\alpha}(x,0) \tag{23}$$

Define the estimation error as

$$\begin{cases} e_1 = \hat{x}_1 - x_1 \\ e_2 = \hat{x}_2 - x_2 \end{cases} \tag{24}$$

where e_1 is the motor-side electrical angle estimation error, and e_2 is the motor-side electrical angular velocity error.

Subtracting (4) from (22), the error equation is obtained as

$$\begin{cases} \dot{e}_1 = e_2 - c_1 \mathrm{sig}(e_1)^{1/2} \\ \dot{e}_2 = a_0 e_2 - h - c_2 \mathrm{sig}(e_1) \end{cases} \tag{25}$$

where $c_1 > 0$ and $c_2 > 0$ are the gains of the FTESO.

Theorem 2 *Choosing appropriate gains c_1 and c_2, the estimation error of (25) converges in finite time, and the estimated lumped disturbance is expressed as:*

$$\lim_{t \to t^*} \hat{h} = a_0 e_2 - c_2 \mathrm{sig}(e_1) \tag{26}$$

Proof 2 *Construct the following Lyapunov function:*

$$V(e_1, e_2) = \bar{\boldsymbol{e}}^{\mathrm{T}} \boldsymbol{Q} \bar{\boldsymbol{e}} \tag{27}$$

where $\bar{\boldsymbol{e}} = \begin{bmatrix} \mathrm{sig}(e_1)^{1/2} & e_2 \end{bmatrix}^{\mathrm{T}}$, $\boldsymbol{Q}$ is a symmetric positive definite matrix.

Let $\boldsymbol{Q} = \begin{bmatrix} q_{11} & q_{12} \\ q_{21} & q_{22} \end{bmatrix}$, and $q_{12} = q_{21}$ and $\det(\boldsymbol{Q}) > 0$. If the parameters of the matrix satisfy $q_{11} > 0$, then the Lyapunov function $V(e_1, e_2)$ is positive definite. The following standard inequality is obtained from (27):

$$\lambda_{min}(\boldsymbol{Q}) \|\bar{\boldsymbol{e}}\|_2^2 \le V(e_1, e_2) \le \lambda_{max}(\boldsymbol{Q}) \|\bar{\boldsymbol{e}}\|_2^2 \tag{28}$$

where $\lambda_{min}(\boldsymbol{Q})$ and $\lambda_{max}(\boldsymbol{Q})$ are the minimum and maximum eigenvalues of the $\boldsymbol{Q}$, respectively.

Then, Equation (29) can be obtained from (28):

$$V^{1/2}(e_1, e_2) / \lambda_{max}^{1/2}(\boldsymbol{Q}) \le \|\bar{\boldsymbol{e}}\|_2 \tag{29}$$

Since $\frac{d[\mathrm{sig}(e_1)^{1/2}]}{dt} = \frac{|e_1|^{-1/2}\dot{e}_1}{2}$, the first order derivative of matrix $\bar{\boldsymbol{e}}$ is

$$\begin{aligned} \dot{\bar{\boldsymbol{e}}} &= \begin{bmatrix} |e_1|^{-1/2}\dot{e}_1/2 & \dot{e}_2 \end{bmatrix}^{\mathrm{T}} \\ &= \begin{bmatrix} |e_1|^{-1/2}\left(e_2 - c_1 sig(e_1)^{1/2}\right)/2 & a_0 e_2 - h + c_2 sig(e_1) \end{bmatrix}^{\mathrm{T}} \\ &= \begin{bmatrix} -\rho c_1/2 & \rho/2 \\ c_2/\rho & a_0 \end{bmatrix} \bar{e} - \begin{bmatrix} 0 \\ 1 \end{bmatrix} h = \boldsymbol{A}\bar{\boldsymbol{e}} + \boldsymbol{B}h \end{aligned} \tag{30}$$

where $\rho = |e_1|^{-1/2}$ is positive.

The characteristic equation of the matrix $\boldsymbol{A}$ is

$$G(s) = s^2 + (\rho c_1/2 - a_0)\, s + (c_2 - a_0 \rho c_1)/2$$

. If $(\rho c_1/2 - a_0) > 0$, $(c_2 - a_0 \rho c_1) > 0$, then we can get that all the coefficients of the polynomial $G(s)$ are positive, and matrix $\boldsymbol{A}$ satisfies the Hurwitz condition, so the error transfer function matrix $\boldsymbol{A}$ is stable.

Taking the first order derivative of (27) yields

$$\begin{aligned} \dot{V}(e_1, e_2) &= \dot{\bar{\boldsymbol{e}}}^{\mathrm{T}} \boldsymbol{Q} \bar{\boldsymbol{e}} + \bar{\boldsymbol{e}}^{\mathrm{T}} \boldsymbol{Q} \dot{\bar{\boldsymbol{e}}} \\ &= (\boldsymbol{A}\bar{\boldsymbol{e}} + \boldsymbol{B}h)^{\mathrm{T}} \boldsymbol{Q} \bar{\boldsymbol{e}} + \bar{\boldsymbol{e}}^{\mathrm{T}} \boldsymbol{Q} (\boldsymbol{A}\bar{\boldsymbol{e}} + \boldsymbol{B}h) \\ &= \bar{\boldsymbol{e}}^{\mathrm{T}} \left(\boldsymbol{A}^{\mathrm{T}}\boldsymbol{Q} + \boldsymbol{Q}\boldsymbol{A}\right) \bar{\boldsymbol{e}} + 2h\tilde{\boldsymbol{B}}^{\mathrm{T}} \bar{\boldsymbol{e}} \end{aligned} \tag{31}$$

where $\tilde{\boldsymbol{B}}^{\mathrm{T}} = -\boldsymbol{B}^{\mathrm{T}}\boldsymbol{Q} = \begin{bmatrix} q_{12} & q_{22} \end{bmatrix}$, $\left\|\tilde{\boldsymbol{B}}\right\|_2 = \sqrt{q_{12}^2 + q_{22}^2}$.

Let $l = \sqrt{q_{12}^2 + q_{22}^2}$, and since $\boldsymbol{A}$ is a Hurwitz matrix, it follows from the properties of Hurwitz matrices that there exists a positive definite matrix $\boldsymbol{P}$, such that $\boldsymbol{Q}$ solves the Lyapunov equation.

Define the positive definite matrix as

$$\boldsymbol{P} = -\left(\boldsymbol{A}^{\mathrm{T}}\boldsymbol{Q} + \boldsymbol{Q}\boldsymbol{A}\right) = -\begin{bmatrix} p_{11} & p_{12} \\ p_{21} & p_{22} \end{bmatrix} \tag{32}$$

where $p_{11} = -\rho c_1 q_{11} + \frac{2c_2}{\rho} q_{12}$, $p_{22} = \rho q_{12} + 2a_0 q_{22}$, $p_{12} = p_{21} = \frac{\rho}{2} q_{11} - \frac{\rho c_1}{2} q_{12} + \frac{c_2}{\rho} q_{22} + a_0 q_{12}$.

Equation (31) can be converted to

$$\begin{aligned} \dot{V}(e_1, e_2) &= -\bar{\boldsymbol{e}}^{\mathrm{T}} \boldsymbol{P} \bar{\boldsymbol{e}} + 2h\tilde{\boldsymbol{B}}^{\mathrm{T}} \bar{\boldsymbol{e}} \\ &\le -\lambda_{min}(\boldsymbol{P}) \|\bar{\boldsymbol{e}}\|_2^2 + 2|h| l \times \|\bar{\boldsymbol{e}}\|_2 \end{aligned} \tag{33}$$

From (28) and (33), we get

$$\begin{aligned} \dot{V}(e_1, e_2) &\le -\frac{\lambda_{min}(\boldsymbol{P})}{\lambda_{max}^{1/2}(\boldsymbol{Q})} \|\bar{\boldsymbol{e}}\|_2 V^{1/2}(e_1, e_2) \\ &\quad + 2|h| l \|\bar{\boldsymbol{e}}\|_2 \\ &\le -\frac{\lambda_{min}(\boldsymbol{P})}{\lambda_{max}^{1/2}(\boldsymbol{Q})} \|\bar{\boldsymbol{e}}\|_2 V^{1/2}(e_1, e_2) + M \end{aligned} \tag{34}$$

where $M = 2|h| l \|\bar{\boldsymbol{e}}\|_2$.

By Lemma 1, when $0 \le g \le 1$, the estimated error converges in finite time. The convergence time is

$$t^* \le \frac{2\lambda_{max}^{1/2}(\boldsymbol{Q})}{g \|\bar{\boldsymbol{e}}\|_2 \lambda_{min}(\boldsymbol{P})} V^{1/2}(e_i, 0)\, (i = 1, 2).$$

When $t < t^*$ and $\forall \rho > 0$, there exists $\left|\hat{h} - h\right| < \rho$; when $t > t^*$, the estimated lumped disturbance is obtained according to (25):

$$\lim_{t \to t^*} \hat{h} = a_0 e_2 - c_2 \mathrm{sig}(e_1) \tag{35}$$

Figures 3 and 4 present the block diagrams of the FTESO and the control of the PMSM dual-inertia system, respectively.

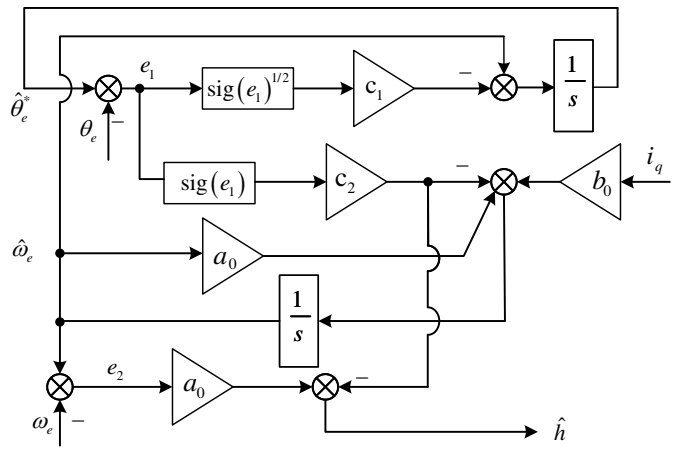

FIGURE 3. Block diagram of FTESO.

5. SIMULATION AND EXPERIMENTATION

5.1. Simulation Results and Analysis

The dual-inertia PMSM model is established by using MATLAB/Simulink to verify the superiority of the proposed scheme. The motor is controlled by $i_d = 0$, and the simulation running time is set to 1.8 s. The sampling period of simulation is 10 µs. Table 1 shows the nominal parameters of the PMSM dual-inertia system, while Table 2 lists the parameters of the three control algorithms, namely, FTESO-based INTSMC (INTSMC+FTESO), conventional ESO-based NTSMC (NTSMC+ESO), and PI controller. Among them, the first two methods use the same acceleration feedback gain $G_{VD} = 2$.

The electrical angular velocity of the motor increases from 200 rad/s to 400 rad/s; at 1.3 s, the load torque increases by 3.5 times. Figs. 5 and 6 show the simulation comparison of the INTSMC+FTESO method with PI control and NTSMC+ESO method.

TABLE 1. Parameters of system.

Parameters	Unit	Values
DC link voltage (U_{dc})	V	350
Rotor PM flux (ψ_r)	Wb	0.171
Stator inductance (L_d)	H	0.00334
Stator inductance (L_q)	H	0.00334
Number of pole pairs (p_n)	pairs	4
Stator resistance (R_s)	Ω	1.9
Rotational Inertia (J_M)	$\mathrm{kg \cdot m^2}$	0.025
Stiffness coefficient (K_s)	$\mathrm{N \cdot m \cdot s/rad}$	300

TABLE 2. Parameters of control schemes.

PI	NTSMC	INTSMC
$P=2$	$k=10$	$\lambda=1338$
$I=650$	$\varepsilon=870$	$\gamma_2=0.48$
	$\gamma_1=0.013$	$k_1=0.993$
		$k_2=4500.5$
		$\eta=2$

Figures 5(a) and 5(b) show the electrical angular velocity curves of the motor side and load side, respectively. It can be seen that:

(i) Both the motor and load-side electrical angular velocities of the PI control and NTSMC+ESO methods exhibit excessive overshooting and slow convergence, whereas the motor-side and load-side electrical angular velocities of the INTSMC+FTESO method achieve fast and stable transition to steady state.

(ii) At 1.3 s, the load torque changes abruptly. The motor-side electrical angular velocity of NTSMC+ESO recovers to a steady state at about 1.308 s with large fluctuation, while the recovery time of the INTSMC+FTESO method is shortened by 90.76% compared to the PI control method and 40% compared to the NTSMC+ESO method. In addition, the load-side electrical angular velocity of INTSMC+FTESO is less affected by the sudden change.

This shows that the INTSMC+FTESO method has better anti-disturbance performance than PI control and NTSMC+ESO methods.

Figures 6(a) and 6(b) show the electrical angular acceleration curves of the motor side and load side, respectively. It can be concluded that:

(i) INTSMC+FTESO control strategy exhibits the most excellent performance, with faster acceleration response speeds on both the motor and load sides than NTSMC+ESO method.

(ii) In contrast, PI control suffers from obvious oscillations and has a slower response speed.

(iii) This indicates that the performance of the PMSM dual-inertia system using INTSMC+FTESO control strategy is more stable.

Figure 7 shows the simulation results of *d*-*q* axis currents, and Fig. 8 shows the output torque curve. It can be seen that INTSMC+FTESO method is more stable in controlling *d*-*q* axis currents and output torque with minimum pulsations and shows better control performance in both transient and steady states.

INTSMC uses FTESO to estimate the disturbances, and NTSMC uses ESO to estimate the disturbances. Fig. 9 shows the electromechanical angular velocity tracking errors of FTESO and ESO. Fig. 10 shows the estimated unknown disturbances of FTESO and ESO.

It can be seen from Fig. 9 that the electrical angular velocity tracking errors of both ESO and FTESO converge in a shorter time. FTESO is less affected by the sudden change of electric angular velocity and load torque, and has better stability performance. It can be seen from Fig. 10 that FTESO provides a more accurate estimation of unknown disturbances and faster tracking response to sudden changes than ESO.

5.2. Experimental Results and Analysis

Figure 11 shows an RT-LAB (OP5600) experimental platform, which is mainly composed of a host computer, digital signal processing (DSP), and OP5600. TMS230F2812 is the control chip of the DSP, and the RT-LAB (OP5600) simulates the

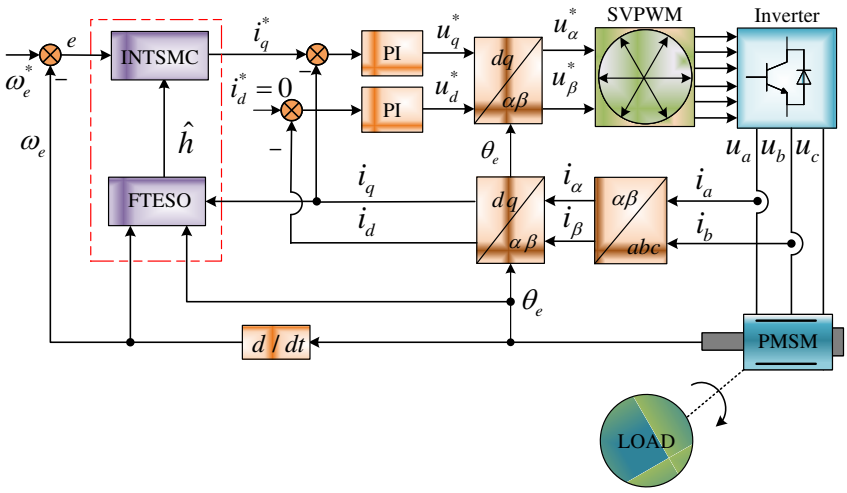

FIGURE 4. Block diagram of PMSM dual-inertia system.

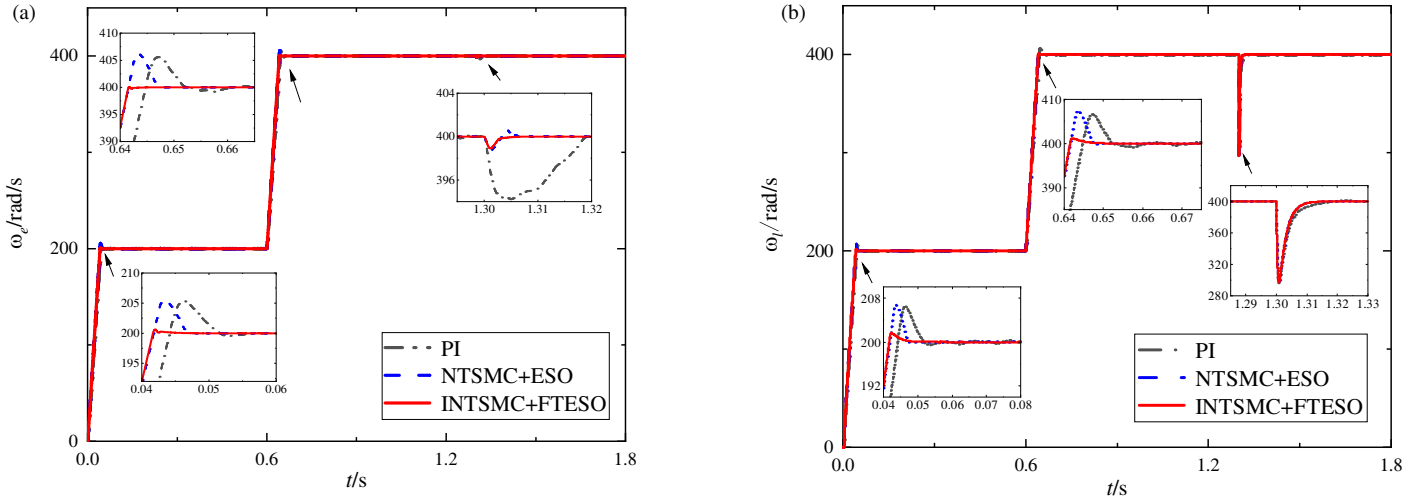

velocity of motor side, ω_e.

velocity of load side, ω_l.

FIGURE 5. Velocity of electrical angular on the motor and load sides.

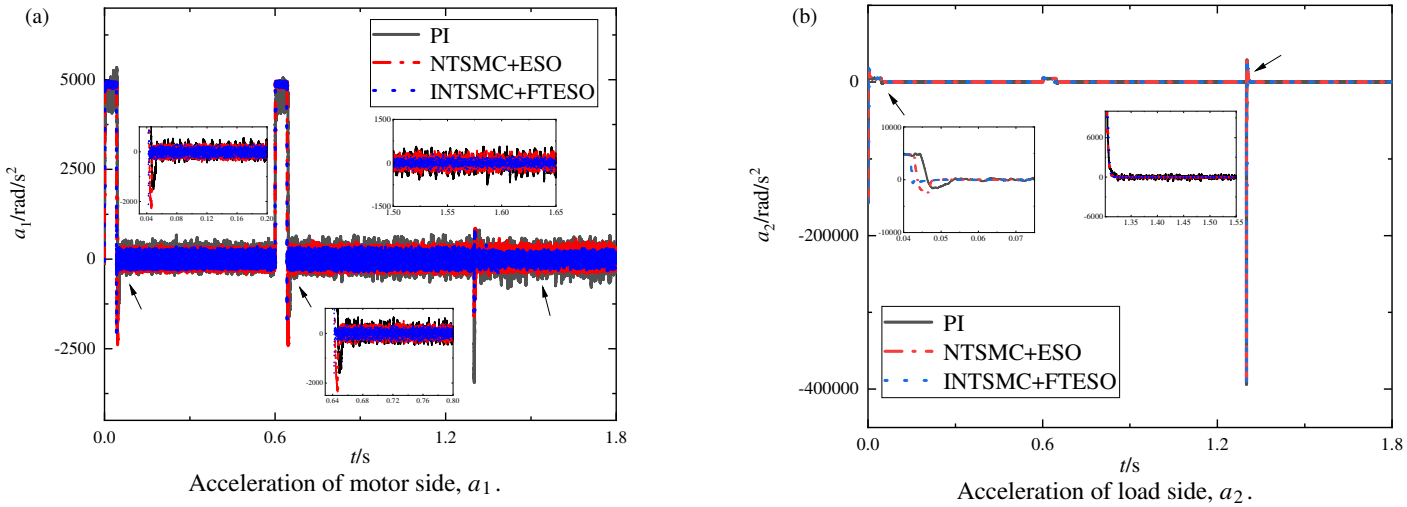

Acceleration of motor side, a_1.

Acceleration of load side, a_2.

FIGURE 6. Acceleration comparison of PI, NTSMC and INTSMC.

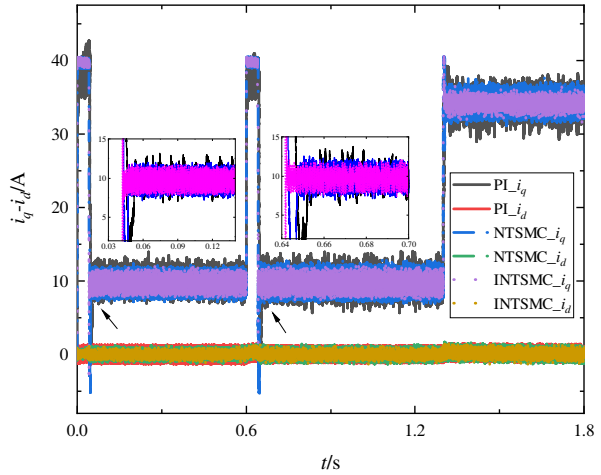

FIGURE 7. d-q axis currents comparison of PI, NTSMC, and INTSMC.

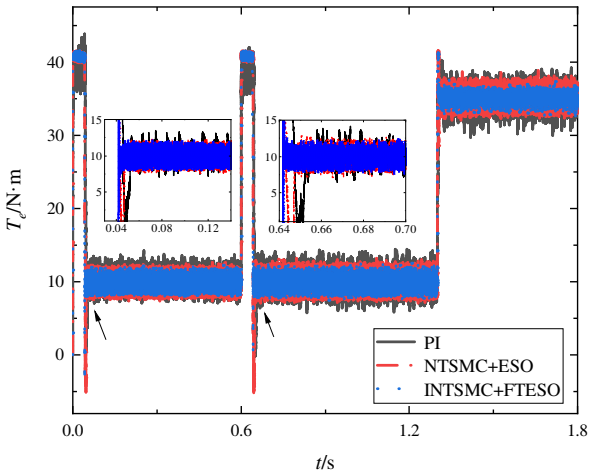

FIGURE 8. Output Torque comparison of PI, NTSMC, and INTSMC.

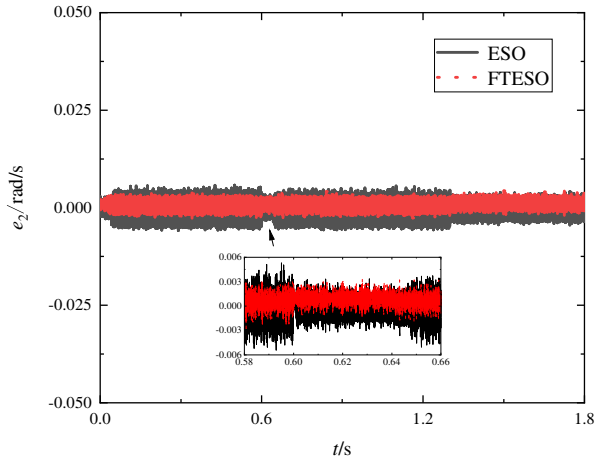

FIGURE 9. Electrical angular velocity tracking errors of ESO and FTESO.

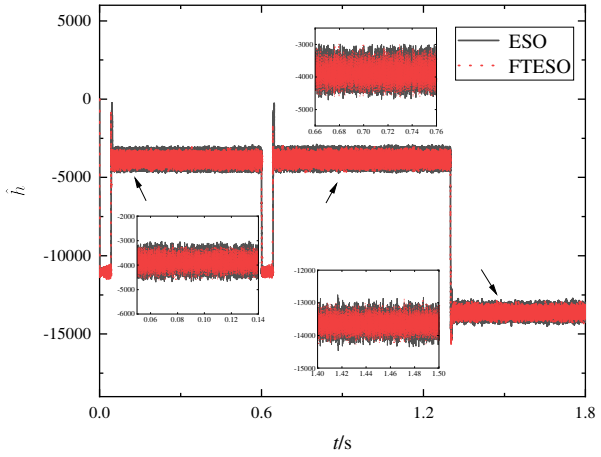

FIGURE 10. Estimation of unknown disturbances by ESO and FTESO.

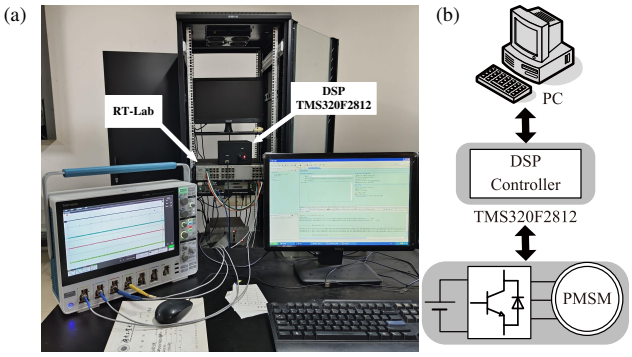

RT-LAB platform. Configuration.

FIGURE 11. RT-LAB (OP5600) experimental platform.

PMSM dual-inertia system. The experimental and simulation parameters are kept consistent.

Figure 12 shows the experimental results of the three methods of PI, NTSMC+ESO, and INTSMC+FTESO, respectively. It can be concluded that:

(i) The designed INTSMC+FTESO method has the fastest electromechanical angular velocity response and the smallest steady error during sudden changes of electric angular velocity and load torque.

(ii) After the load torque is increased to 35 $N \cdot m$, PI and NTSMC+ESO methods have deficiencies in anti-disturbance performance and convergence speed, while INTSMC+FTESO method has the smallest current fluc-

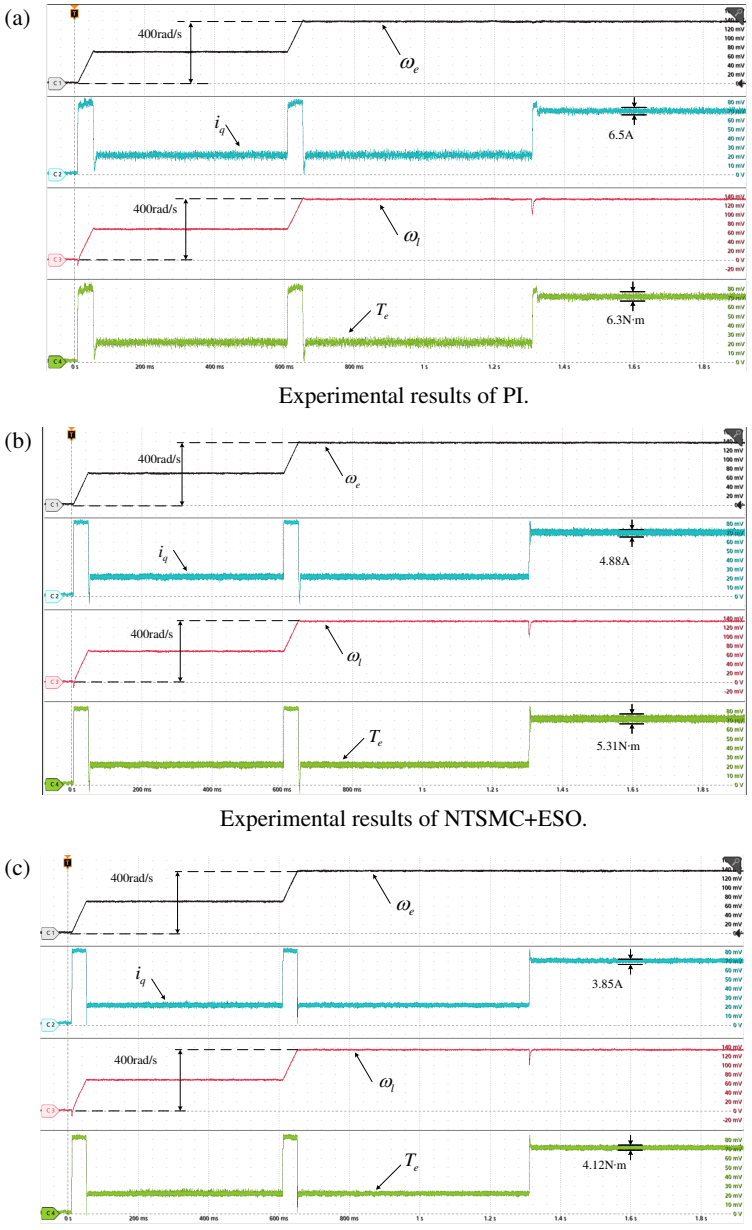

FIGURE 12. Experimental results of PI, NTSMC+ESO, and INTSMC+FTESO.

tuation; the output torque is more stable; and it performs excellently in dynamic response and steady state.

6. CONCLUSION

Aiming at the problem of control performance degradation caused by unknown disturbances in the PMSM dual-inertia system, this paper proposes an INTSMC approach based on FTESO. The proposed INTSMC+FTESO method was compared with PI control and NTSMC+ESO methods. The following conclusions are drawn:

(i) The dual-inertia model of a PMSM-driven flexible load system is developed. The INTSMC is designed using a new reaching law that adaptively adjusts the convergence speed. It achieves an effective balance between the system convergence speed and chattering attenuation.

(ii) The designed FTESO estimates the interference and performs accurate feed-forward compensation for the INTSMC to ensure the robustness of the system.

(iii) By comprehensive comparison with PI control and NTSMC+ESO method, it is verified that FTESO+INTSMC method has better anti-disturbance capability and effectively suppresses current and torque pulsations.

Developing cascaded ESOs to classify and compensate disturbances is a promising strategy. In the future, we will apply it to PMSM dual-inertia system.

ACKNOWLEDGEMENT

This work was supported by the National Natural Science Foundation of China under Grant Number (62303178), and the Natural Science Foundation of Hunan Province Number (2023JJ50193 and 2024JJ7139).

REFERENCES

[1] Jia, N., K. Zhao, Y. Lv, and X. Li, "Non-singular fast terminal sliding mode control torsional vibration suppression for PM synchronous transmission system of EVs," *Progress In Electromagnetics Research M*, Vol. 122, 63–72, 2023.

[2] Wang, B., M. Tian, Y. Yu, Q. Dong, and D. Xu, "Enhanced ADRC with quasi-resonant control for PMSM speed regulation considering aperiodic and periodic disturbances," *IEEE Transactions on Transportation Electrification*, Vol. 8, No. 3, 3568–3577, Sep. 2022.

[3] Madonski, R., M. Stanković, S. Shao, Z. Gao, J. Yang, and S. Li, "Active disturbance rejection control of torsional plant with unknown frequency harmonic disturbance," *Control Engineering Practice*, Vol. 100, 104413, Jul. 2020.

[4] Śleszycki, K., K. Wróbel, K. Szabat, and S. Katsura, "Parameter identification of the two-mass system with the help of multi-layer estimator," in *2021 IEEE 30th International Symposium on Industrial Electronics (ISIE)*, 1–6, Kyoto, Japan, Jun. 2021.

[5] Wang, B., M. Iwasaki, and J. Yu, "Command filtered adaptive backstepping control for dual-motor servo systems with torque disturbance and uncertainties," *IEEE Transactions on Industrial Electronics*, Vol. 69, No. 2, 1773–1781, Feb. 2022.

[6] Sun, L., X. Li, L. Chen, H. Shi, and Z. Jiang, "Dual-motor coordination for high-quality servo with transmission backlash," *IEEE Transactions on Industrial Electronics*, Vol. 70, No. 2, 1182–1196, 2023.

[7] Lu, Y., K. Zhao, X. You, M. Qiao, Y. He, and L. Tu, "Model-free recursive terminal sliding mode control for a permanent magnet synchronous motor dual inertia system based on a double disturbance observer," *Power System Protection and Control*, Vol. 52, No. 21, 129–139, 2024.

[8] Shao, K., J. Zheng, C. Yang, F. Xu, X. Wang, and X. Li, "Chattering-free adaptive sliding-mode control of nonlinear systems with unknown disturbances," *Computers & Electrical Engineering*, Vol. 96, 107538, 2021.

[9] Shao, K., "Nested adaptive integral terminal sliding mode control for high-order uncertain nonlinear systems," *International Journal of Robust and Nonlinear Control*, Vol. 31, No. 14, 6668–6680, 2021.

[10] Hou, H., X. Yu, L. Xu, R. Chuei, and Z. Cao, "Discrete-time terminal sliding-mode tracking control with alleviated chattering," *IEEE/ASME Transactions on Mechatronics*, Vol. 24, No. 4, 1808–1817, 2019.

[11] Yu, X., Y. Feng, and Z. Man, "Terminal sliding mode control — An overview," *IEEE Open Journal of the Industrial Electronics Society*, Vol. 2, 36–52, 2020.

[12] Xu, D., B. Ding, B. Jiang, W. Yang, and P. Shi, "Nonsingular fast terminal sliding mode control for permanent magnet linear synchronous motor via high-order super-twisting observer," *IEEE/ASME Transactions on Mechatronics*, Vol. 27, No. 3, 1651–1659, Jun. 2022.

[13] Kang, E., H. Yu, and K. Han, "Nonlinear gain non-singular fast terminal sliding mode control for permanent magnet synchronous motors," *Electric Machines and Control*, Vol. 28, No. 5, 73–81, 2024.

[14] Jiang, F., S. Sun, A. Liu, Y. Xu, Z. Li, X. Liu, and K. Yang, "Robustness improvement of model-based sensorless SPMSM drivers based on an adaptive extended state observer and an enhanced quadrature PLL," *IEEE Transactions on Power Electronics*, Vol. 36, No. 4, 4802–4814, Apr. 2021.

[15] Wang, M., Y. Liu, Q. Wang, Y. Liao, and P. Wheeler, "Speed-current single-loop control of PMSM based on model-assisted cascaded extended state observer and sliding mode control," *International Journal of Circuit Theory and Applications*, Vol. 52, No. 7, 3558–3583, Jul. 2024.

[16] Yang, J., Y. Ye, Y. Cheng, and L. Hua, "Nonsingular terminal sliding mode control of the yarn winding process based on a finite-time extended state observer," *IEEE Access*, Vol. 13, 21 610–21 619, 2025.

[17] Hou, Q. and S. Ding, "Finite-time extended state observer-based super-twisting sliding mode controller for PMSM drives with inertia identification," *IEEE Transactions on Transportation Electrification*, Vol. 8, No. 2, 1918–1929, Jun. 2022.

[18] Zhang, X., W. Xue, Z. Liu, R. Zhang, and H. Li, "Compensated acceleration feedback based active disturbance rejection control for launch vehicles," *Chinese Journal of Aeronautics*, Vol. 37, No. 4, 464–478, 2024.

[19] Yu, J., Y. Feng, and J. F. Zheng, "Suppression of mechanical resonance based on higher-order sliding mode and acceleration feedback," *Control Theory & Applications*, Vol. 26, No. 10, 1133–1136, 2009.

[20] Hou, Q. and S. Ding, "Finite-time extended state observer-based super-twisting sliding mode controller for pmsm drives with inertia identification," *IEEE Transactions on Transportation Electrification*, Vol. 8, No. 2, 1918–1929, Jun. 2022.

[21] Wang, H., B. Chen, C. Lin, Y. Sun, and F. Wang, "Adaptive finite-time control for a class of uncertain high-order non-linear systems based on fuzzy approximation," *IET Control Theory & Applications*, Vol. 11, No. 5, 677–684, 2017.